

Differentiation of benign and malignant focal liver lesions: value of virtual touch tissue quantification of acoustic radiation force impulse elastography

Le-Hang Guo · Shu-Jun Wang · Hui-Xiong Xu ·
Li-Ping Sun · Yi-Feng Zhang · Jun-Mei Xu ·
Jian Wu · Hui-Jun Fu · Xiao-Hong Xu

Received: 3 February 2015 / Accepted: 13 February 2015 / Published online: 19 February 2015
© Springer Science+Business Media New York 2015

Abstract The purpose of this study was to investigate the value of virtual tissue quantification (VTQ) of acoustic radiation force impulse elastography for the differential diagnosis of benign and malignant focal liver lesions (FLLs). Thus, a total of 134 FLLs in 134 patients were included. VTQ measurement was performed for each lesion in which the shear wave velocity (SWV) was measured. The difference in SWV and SWV ratio of FLL to surrounding liver between malignant and benign FLLs was evaluated, and the cutoff value was investigated. Receiver operating characteristic (ROC) curve was plotted to evaluate the diagnostic performance. A total of 134 lesions including 55 (41.0 %) malignant FLLs and 79 (59.0 %) benign ones were analyzed. The SWV of malignant and benign FLLs was 2.95 ± 1.00 m/s and 1.69 ± 0.89 m/s, respectively. Significant difference in SWV was presented between malignant and benign FLLs ($p < 0.001$). The

SWV ratio of each FLL to the surrounding liver parenchyma was 1.83 ± 1.32 for malignant and 1.26 ± 0.78 for benign FLLs ($p < 0.001$). The area under the ROC curve in distinguishing malignant from benign lesions was 0.824 for SWV and 0.660 for SWV ratio. The cutoff value for differential diagnosis was 2.13 m/s for SWV and 1.37 for SWV ratio. The associated sensitivity and specificity were 83.3 and 77.9 % for SWV and 59.6 and 77.3 % for SWV ratio, respectively. In conclusion, VTQ provides quantitative stiffness information of FLLs and is helpful in the differential diagnosis between malignant and benign FLLs, particularly for the patients who are not candidates for contrast-enhanced imaging such as CT, MRI or contrast-enhanced ultrasound.

Keywords Acoustic radiation force impulse · Virtual touch quantification · Shear wave velocity · Focal liver lesion

Le-Hang Guo and Shu-Jun Wang have contributed equally to this manuscript.

L.-H. Guo · S.-J. Wang · H.-X. Xu (✉) · L.-P. Sun ·
Y.-F. Zhang · J.-M. Xu · J. Wu
Department of Medical Ultrasound, Shanghai Tenth People's
Hospital, Tenth People's Hospital of Tongji University,
Shanghai 200072, China
e-mail: xuhuixiong@hotmail.com

H.-J. Fu
Department of Pathology, Shanghai Tenth People's Hospital,
Tenth People's Hospital of Tongji University, Shanghai 200072,
China

X.-H. Xu (✉)
Department of Ultrasound, Guangdong Medical College
Affiliated Hospital, Zhanjiang 524001, China
e-mail: 13828297586@139.com

Introduction

Focal liver lesions (FLLs) are common findings during routine abdominal examinations. Conventional ultrasound (US) is used as the first imaging modality to evaluate FLLs. Although magnetic resonance imaging (MRI), computed tomography (CT) and contrast-enhanced ultrasound (CEUS) have a high-level diagnostic accuracy in assessing the morphology of a FLL [1–4], there are some limitations for each technology. Patients who have any metallic materials within the body (artificial joints, heart pacemakers, artificial heart valves, etc.) cannot be scanned with MRI because of the risk that the magnet may move the metal in these areas [5]. The CT scan will expose patients to radiation hazards [6].

Furthermore, the enhanced CT scan might introduce contrast medium-induced side effects. Patients with unstable cardiopulmonary status, including patients with unstable angina, acute myocardial infarction, respiratory failure or recent congestive heart failure, are the contraindications of CEUS. In addition, CEUS is not applicable to the pregnant or lactating women [7].

Acoustic radiation force impulse (ARFI) elastography has been introduced as a new US modality, which uses focused ultrasound to produce shear waves in the tissue [8]. It provides information about the local mechanical properties of tissue quantitatively and noninvasively [9, 10]. Instead of applying pressure manually to the surface of the specific organ as shown in conventional US elastography, ARFI produces localized displacements in tissue using acoustic pulse [11, 12]. When ARFI imaging is undergoing, tissue is mechanically excited by using short-duration acoustic pulse to generate small (1–10 μm) localized tissue displacements, and the displacement response can be ultrasonically tracked through time [13, 14]. ARFI elastography includes two technologies that are named as virtual touch tissue (VTI) and virtual touch tissue quantification (VTQ). The VTI looks at the displacement amplitudes caused by an acoustic push, whereas VTQ uses the same acoustic push but looks at the displacements lateral to the push to examine how fast the resulting shear wave propagates. This study focused on investigating the application of VTQ in differentiating benign from malignant FLLs. By measuring the time to peak displacement at each lateral location, the shear wave velocity (SWV, m/s) within the region of interest (ROI) can be calculated. ARFI elastography obtains SWV with a metering box of the ROI at variable depth, allowing the examination of specific liver areas [15]. Its quantitative implementation is named as VTQ which provides an objective numerical evaluation of the tissue elastic properties [11, 16]. ARFI elastography has been performed in the tissue such as breast, thyroid, kidney, and pancreas [17–21]. The other clinical application of this approach is noninvasive quantification of liver stiffness in the setting of fibrosis, cirrhosis and steatosis [22–26]. Sporea et al. [24] found that there was a statistically significant correlation between histological fibrosis and ARFI measurement, and the best performance of this method was in the prediction of severe fibrosis and cirrhosis. The clinical application of VTQ has also been expanded to characterize the focal liver masses beyond merely assess liver fibrosis.

In recent years, there have been some studies in investigating the potential usefulness of ARFI elastography to differentiate focal hepatic masses with the wide range of sensitivities (from 81.3 to 97.1 %) and specificities (from 81 to 100 %) [27–33]. However, some of them only evaluated the value of ARFI in distinguishing hemangiomas from

metastases [28] or in differentiating hemangiomas from malignant tumors [33]. In addition, all the previous studies investigated the differential diagnostic value of VTQ in liver masses by absolute value of SWV, and the influence of adjacent liver tissue was not considered. To our knowledge, no study applied the SWV ratio of SWV of FLL to that of its surrounding liver tissue to evaluate the diagnostic value of VTQ. This study aimed to investigate the diagnostic performance of VTQ for distinguishing malignant from benign liver lesions by using the SWV of FLL and the SWV ratio of FLL to that of its surrounding liver parenchyma.

Materials and methods

Subjects and study design

This prospective study was carried out from January 2013 to August 2013. A total of 155 consecutive patients were referred to ARFI examination after one or more FLLs were detected on conventional US. The enrollment criteria were as follows: (1) FLLs detected on conventional US; (2) solid or almost solid lesions based on US findings; and (3) the depth of the lesion was less than 8 cm from body surface. Twenty-one patients were excluded from the study, and the exclusion criteria were as follows: (1) with lesion smaller than the size of the sampling box for SWV measurement ($n = 4$); (2) data loss ($n = 7$); (3) poor image quality (e.g., patient inability to hold breath as required or the lesions were too close to the heart) ($n = 6$); and (4) treatment such as biopsy or ablation was performed on the lesions before ($n = 4$). Finally, 134 patients with valid SWV measurements on ARFI were included. Regarding the patient who had multiple FLLs, only the most conspicuous one on US was chosen (Fig. 1). The mean age of the included patients was 53.1 ± 12.3 years (range 22–79 years). There were 64 men and 70 women. The mean diameter of the lesions was 43.7 ± 25.6 mm (range 10–159 mm). The clinical investigation was conducted according to the principles expressed in the Declaration of Helsinki. The study was approved by the Ethical Committee of the University Hospital, and informed consent was obtained from all the patients.

ARFI elastography

ARFI elastography was performed with Acuson S2000 US system (Siemens Medical Solutions, Mountain View, CA, USA), equipped with a 4-1-MHz convex array probe. The ARFI technique was commercially available and was routinely used in clinical settings.

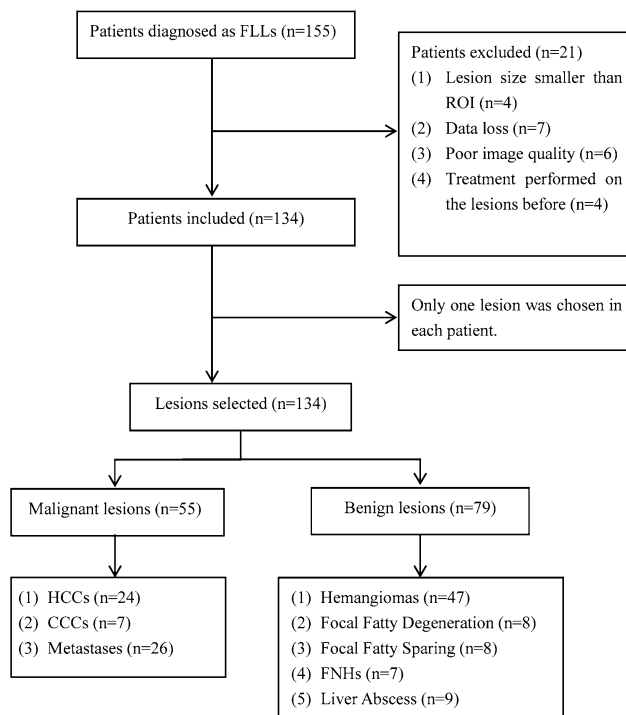


Fig. 1 Flowchart of the selection of the FLLs

All the ARFI elastography was operated by a single radiologist who had more than 3 years of experience in ARFI elastography. After the target lesion was identified by conventional B-mode US imaging, it was placed in the center of the screen with sufficient surrounding liver tissue simultaneously. Then, the image settings were optimized to obtain high-quality image. Subsequently, the patient was asked to hold breath and ARFI elastography was started to measure. The probe was placed gently on the body surface with light pressure on the liver when performing ARFI. The ROI was characterized by a box with a fixed size of 10 mm × 6 mm and was entirely located in the solid portion of the lesion excluding any vascular or biliary structures. The presence of degeneration, such as necrotic, cystic or calcified portions, was not included in the ROI. The ARFI measurement was activated, and the SWV value (in m/s) was displayed on the screen. The measurement was repeated for seven times. Afterwards, the ROI cursor was moved to the surrounding liver tissue at the same depth about 2–3 cm away from the target lesion, and the measurement was repeated for seven times. The minimum and maximum values were eliminated, and the mean of the rest five measurements was conducted for the data analysis. The whole procedure was performed for each patient about 5–10 min without any additional cost and inconvenience for all patients. According to the data provided by Siemens Corporation, the range for the SWV is 0.5–5.00 m/s in abdomen measurement. The value of out of the range is

displayed as “x.xx m/s,” which means not applicable (NA). In other words, both extremely hard and soft tissues are shown as “x.xx m/s.” After excluding the possible influencing factors such as patient’s respiration and operator’s inappropriate gesture, the value of “x.xx m/s” was allocated to be 0.5 m/s (corresponding cystic portion) or 5.00 m/s (corresponding solid portion). The SWV ratio of each FLL to surrounding liver parenchyma was also calculated.

Final diagnoses and reference standard

The final diagnoses of the FLLs were determined by clinical diagnoses or histological diagnoses. There were 11 patients confirmed by pathological examination with specimens obtained from surgery, and the remaining patients were diagnosed by clinical data, patient history and other imaging modalities (CT or MRI). For the patients without pathological results, the recent guidelines were referenced, and all the data of the patients were reviewed by a senior radiologist who had more than 19 years of experience in liver imaging. A clinical diagnosis of hepatocellular carcinoma (HCC) was made according to the American Association for the Study of Liver Disease (AASLD) recommendation that typical findings of arterial hypervascularity and subsequent washout were documented on dynamic CT or MRI in patients with liver cirrhosis [34, 35]. The cholangiocellular carcinomas (CCCs) were all confirmed by pathological examination. Metastases were confirmed by pathological results of the origin tumors, newly detected lesions in the liver and typical findings on contrast-enhanced CT or MRI. According to the previous literature, the benign lesions such as hemangioma, focal fatty degeneration, focal fatty sparing and focal nodular hyperplasia (FNH) were confirmed by typical imaging findings on contrast-enhanced CT or MRI.

Hemangiomas were confirmed by the typical findings of peripheral or complete homogeneous fill-in from arterial phase to portal venous phase and hypo-enhanced in delay phase [36, 37]. FNH has a fairly consistent appearance in MRI, which was iso-intense (except for a central scar) and indistinguishable from normal hepatic parenchyma on all pulse sequences [38]. Focal fatty degeneration and focal fatty sparing were confirmed by the background of fatty liver disease and the iso-enhancement with the surrounding hepatic parenchyma; besides, no change in size, shape and echogenicity for all the lesions was found in a US follow-up over 1 year. Liver abscess was confirmed by percutaneous drainage or imaging follow-up.

Finally, the malignant lesions included HCC ($n = 24$), CCC ($n = 5$) and metastases ($n = 26$; seven from colon cancers, two from rectal cancers, five from pancreatic cancers, four from gastric stromal tumors, three from

gallbladder cancers, three from breast cancers, one from ovarian cancer and one from esophagus cancer). Benign lesions included hemangioma ($n = 47$), focal fatty degeneration ($n = 8$), focal fatty sparing ($n = 8$), liver abscess ($n = 9$) and FNH ($n = 7$).

Statistical analysis

The SPSS version 18.0 software package for Windows (SPSS Inc, Chicago, IL) was used for statistical analysis of the data. Continuous variables were expressed as mean \pm standard deviation (SD) and ranges. The χ^2 test was used to compare categorical variables. The differences between the SWV of FLLs and their surrounding liver parenchyma were analyzed with independent t test. The differences among the SWV of each type of FLLs were evaluated with analysis of variance (ANOVA) test. Receiver operating characteristics (ROC) curve and areas under the ROC (AUROC) were used to estimate the diagnostic performance. The cutoff value was defined by considering the highest sum of sensitivity and specificity. p value < 0.05 was considered as statistically significant.

Results

A total of 134 lesions [55 (41.0 %) malignant lesions and 79 (59.0 %) benign lesions] were assessed. The mean age of the patients was 53.1 ± 12.3 years (range 22–79 years), including 64 male and 70 female. There was significant difference between the mean age of patients with malignant masses (61.6 ± 9.2 years, range 37–79 years) and the mean age of patients with benign lesions (50.4 ± 13.1 years, range 22–79 years) ($p < 0.001$).

In the patients with malignant masses, there were 33 men and 24 women. There were 40 men patients and 57 women patients with benign lesions. There was gender significant difference between the malignant and benign lesions. The mean diameter of the lesions was 43.7 ± 25.6 mm (range 10–159 mm). There was statistically significant difference between the mean diameter of malignant masses (54.4 ± 34.3 mm, range 13–159 mm) and the mean diameter of benign ones (33.1 ± 22.7 mm, range; 11–108 mm). The SWVs were 3.07 ± 0.89 m/s (range 1.53–5.00 m/s) in HCCs (Fig. 2), 3.44 ± 1.18 m/s (range 2.27–5.00 m/s) in CCCs, 2.74 ± 1.06 m/s (range 0.72–4.73 m/s) in metastases (Fig. 3), 1.48 ± 0.70 m/s (range 0.69–3.68 m/s) in hemangiomas (Fig. 4), 1.71 ± 0.65 m/s (range 0.95–2.64 m/s) in focal fatty degenerations, 1.51 ± 1.15 m/s (range 0.81–4.33 m/s) in focal fatty sparing, 2.46 ± 0.98 m/s (range 1.29–3.90 m/s) in liver abscess and 2.30 ± 1.18 m/s (range 1.02–4.44 m/s) in FNH, respectively.

The SWV values for metastases and FNHs were significantly higher than those for their surrounding liver parenchyma ($p < 0.05$). However, the SWV values of the other FLLs were similar to those for their surrounding liver parenchyma. The SWVs of FLLs, surrounding liver parenchyma and the SWV ratios of FLLs to surrounding liver tissues are presented in Table 1.

A full matrix of pairwise comparison between all the lesions was made. The SWV of HCCs was 3.07 ± 0.89 m/s (range 1.53–5.00 m/s), which was significantly higher than focal fatty degeneration (1.71 ± 0.65 m/s, range 0.95–2.64 m/s, $p = 0.006$) and hemangioma (1.48 ± 0.70 m/s, range 0.69–3.68 m/s, $p < 0.001$). The SWV of metastases was 2.74 ± 1.06 m/s (range 0.72–4.73 m/s), which was significantly higher than hemangioma ($p < 0.001$). The SWV value of the surrounding liver of HCC was higher than the surrounding liver of other lesions ($p < 0.05$), except the surrounding liver of CCC ($p = 0.986$) and abscess ($p = 0.637$) (Table 1).

The HCCs, CCCs and metastases were categorized into a malignant liver mass group ($n = 55$), and the others were classified into a benign lesion group ($n = 79$). The SWVs of malignant and benign FLLs were 2.95 ± 1.00 m/s (range 0.72–5.00 m/s) and 1.69 ± 0.89 m/s (range 0.69–4.44 m/s), respectively. The SWV ratios of FLLs to their surrounding liver tissues were 1.83 ± 1.32 (range 0.39–6.43) for the malignant FLLs and 1.26 ± 0.78 (range 0.33–5.73) for the benign ones (Table 1).

The AUROC for the SWV was 0.824 (95 % CI 0.748–0.899) and 0.660 (95 % CI 0.555–0.765) for the SWV ratio in discriminating malignant from benign FLLs (Figs. 5, 6). The corresponding sensitivity, specificity, positive predictive value (PPV) and negative predictive value (NPV) for SWV and SWV ratio are presented in Fig. 5. The best cutoff value was 2.13 m/s for SWV and 1.37 for SWV ratio in distinguishing malignant lesions from benign ones.

Discussion

Consistent with previous studies [27–33], the mean SWV of malignant liver masses (2.95 m/s) in our study was higher than that of benign lesions (1.68 m/s). This finding indicates that malignant liver masses were harder than benign ones. The mean SWV of HCCs in our study was 3.07 m/s, which was higher than that of above-mentioned studies (2.45–2.66 m/s), whereas the SWVs of metastases (2.74 m/s) and CCCs 3.44 m/s were close to their reports (2.18–3.20 m/s in metastases, 1.65–3.74 m/s in CCC) [27, 30–33]. These results were likely due to the constitution of pathological tissues. FLLs with more fibrous tissue are potentially stiffer, but FLLs with more vascular component

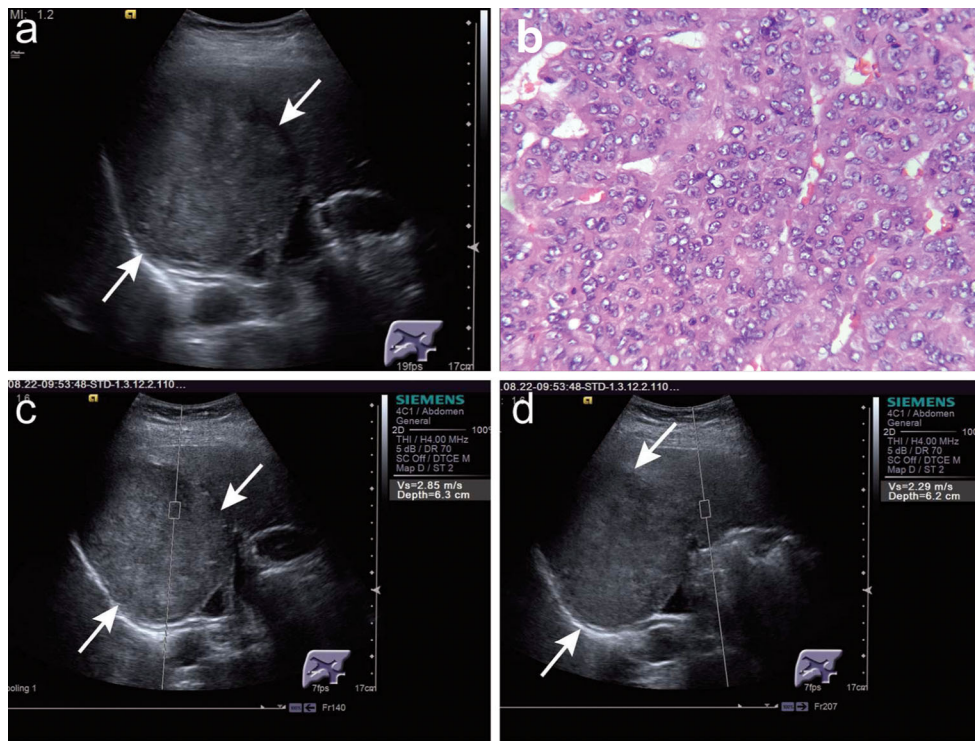


Fig. 2 A 49-year-old woman with an HCC. **a** B-mode US image of the lesion. **b** Microscopically, abundant hepatocytes arranged densely. **c** VTQ of the lesion shows the SWV is 2.85 m/s. **d** The SWV of the surrounding liver parenchyma is 2.29 m/s

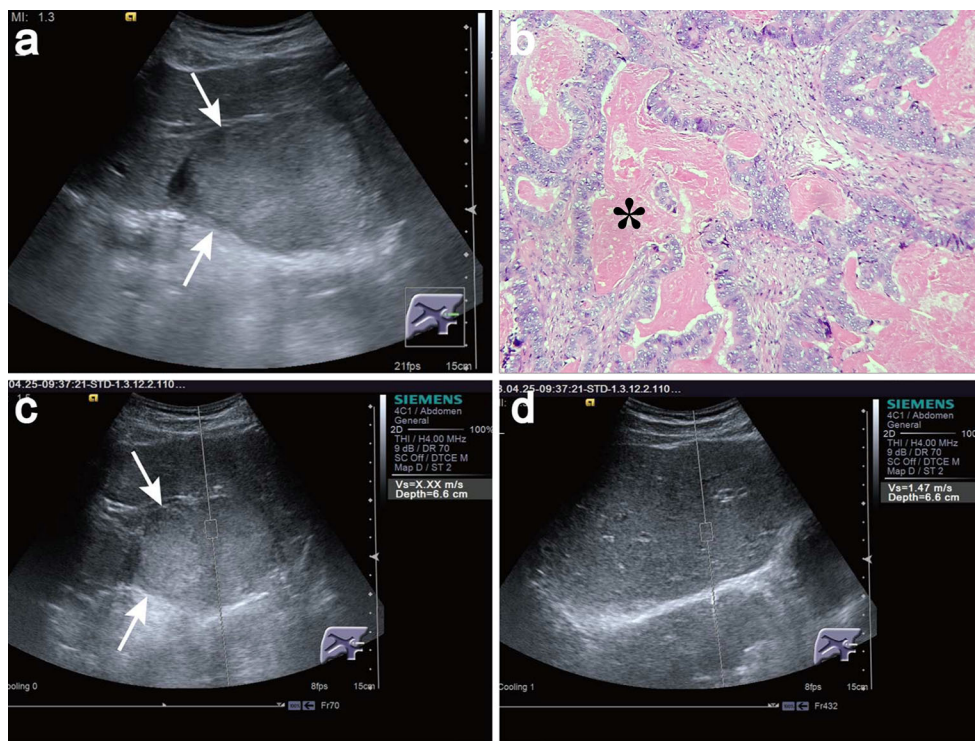


Fig. 3 A 59-year-old man with a metastasis liver cancer (originated from colon cancer). **a** B-mode US image of the lesion. **b** Microscopically, massive necrosis (*) was observed markedly among the tumors. **c** VTQ of the lesion shows the SWV is displayed as x.xx m/s (i.e., 5 m/s). **d** The SWV of the surrounding liver parenchyma is 1.47 m/s

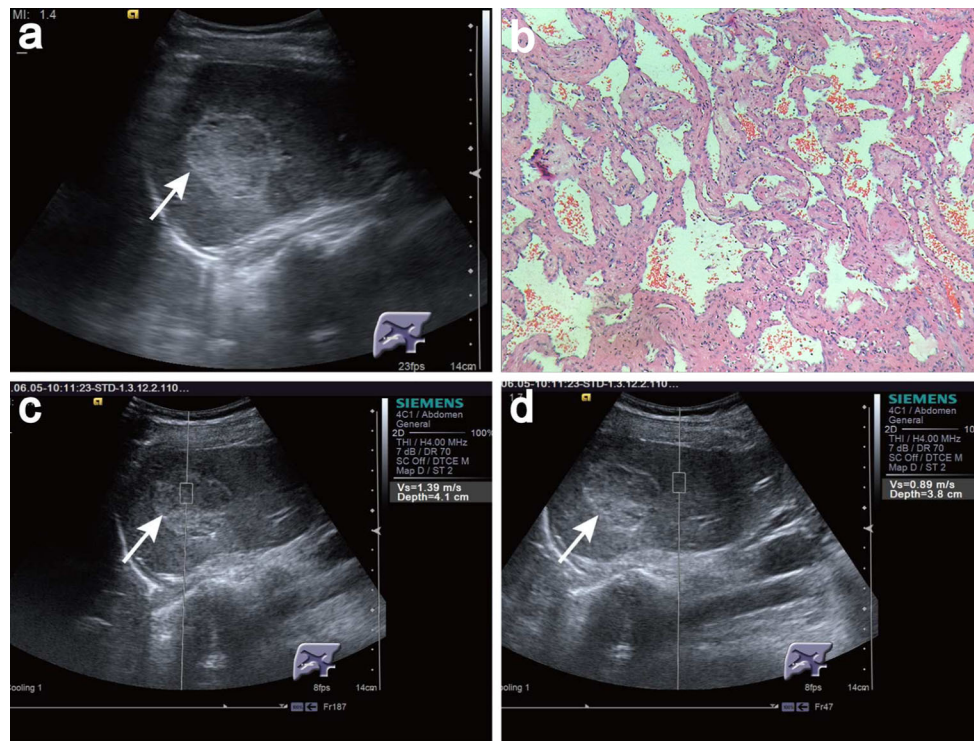


Fig. 4 A 39-year-old woman with a hemangioma. **a** B-mode US image of the lesion. **b** Microscopically, hemangiomas composed by multiple circuitous vascular sinus. **c** VTQ of the lesion shows the SWV is 1.39 m/s. **d** The SWV of the surrounding liver parenchyma is 0.89 m/s

tend to be softer [30]. CCC is comparatively the hardest lesion because it is rich in fibrotic tissue instead of vessels. HCC is composed of hepatocytes, rich vessels and less fibrotic tissue, which makes it relatively softer than CCC. A larger-scale study with increased sample size and exact comparison between the HCCs and CCCs should be performed in the future. Stiffness of metastasis depends on the amount of fibrous and vessels of the tumor.

The mean SWV for hemangiomas was 1.48 m/s with a wide range of 0.69–3.68 m/s in this study. It was comparable to the other two previous studies (1.51 and 1.35 m/s) [27, 28], whereas the values in other reports were higher (2.36, 1.83 and 1.80 m/s) [31–33]. Why hemangiomas have such a variation in stiffness may be explained by the pathological spectrum of hemangiomas. Hemangiomas are composed of cavernous vascular spaces of varying sizes lined by a single layer of flat endothelium and separated by thin fibrous septa. Thus, hemangiomas composed by multiple circuitous vascular sinus filled with blood would be expected to be soft ideally, which means they would have low SWVs. In contrast, hemangiomas contain various amounts of fibrous septa or include pathological degeneration such as thrombosis or calcification would be stiff and have high SWVs [12]. In other word, the variability in SWVs for hemangiomas might be based on the amount of fibrous septa that divide the dilated sinusoid [27]. The

mean SWV for FNHs (2.30 m/s) in our study was significantly different from other two studies, which was 1.90 m/s [30] and 0.97 m/s [32], respectively. This discrepancy may because of great disparity of sample size in each study. The primary components of FNH are hyperplastic hepatic cells and vessels except for the central scar; thus, it tends to be relatively softer than malignant lesions.

For the differential diagnosis of FLLs, the underlying background of liver fibrosis should not be overlooked. Some previous studies proposed that HCCs generally appeared relatively softer than the surrounding liver tissue and the stiffness of HCC decreased with increasing hepatic parenchymal fibrosis grade [39, 40], whereas metastases and hemangiomas generally appeared harder than the adjacent liver parenchyma [32, 39, 40]. Our results about comparing HCCs and hemangiomas to their surrounding liver parenchyma seemed to be inconsistent with the above reports. In our study, the SWVs for HCCs and hemangiomas were equivalent to those of their surrounding liver parenchyma. However, the SWVs for metastases and FNHs were higher than those of their surrounding liver tissue. Since metastases and FNHs were encountered in patients without underlying chronic liver disease in most situations, the SWVs seemed to be consistently higher than those of background liver. On the contrary, HCCs were always encountered in patients with underlying chronic liver

Table 1 SWVs of FLLs and the SWV ratios of FLLs to surrounding liver parenchyma

	Lesion no	SWV of lesions (m/s)	SWV of surrounding tissue(m/s)	SWV ratio	<i>p</i> ^a
All	134	2.37 ± 1.51 (0.69–5.00)	1.74 ± 1.06 (0.69–5.00)	1.48 ± 1.05 (0.33–6.43)	<0.001
Malignant	55	2.95 ± 1.00 (0.72–5.00)	2.00 ± 0.98 (0.69–5.00)	1.83 ± 1.32 (0.39–6.43)	<0.001
HCC	24	3.07 ± 0.89 ^b (1.53–5.00)	2.72 ± 0.83 ^c (1.72–5.00)	1.29 ± 0.84 (0.46–6.23)	0.141
CCC	5	3.44 ± 1.18 (2.27–5.00)	2.20 ± 0.92 (1.28–3.58)	1.71 ± 0.59 (0.76–2.23)	0.099
Metastasis	26	2.74 ± 1.06 ^b (0.72–4.73)	1.85 ± 0.84 ^c (0.69–3.87)	1.76 ± 1.32 (0.39–6.43)	0.003
Benign	79	1.68 ± 0.88 (0.69–4.44)	1.49 ± 0.75 (0.72–4.09)	1.26 ± 0.78 (0.33–5.73)	0.157
Hemangioma	47	1.48 ± 0.70 ^b (0.69–3.68)	1.51 ± 0.80 ^c (0.72–4.09)	1.09 ± 0.48 (0.33–3.10)	0.833
Focal fatty degeneration	8	1.71 ± 0.65 ^b (0.95–2.64)	1.39 ± 0.50 ^c (0.78–2.13)	1.24 ± 0.23 (0.89–1.57)	0.279
Focal fatty sparing	8	1.51 ± 1.15 (0.81–4.33)	1.26 ± 0.34 ^c (0.76–1.84)	1.45 ± 1.73 (0.64–5.73)	0.577
FNH	7	2.30 ± 1.18 (1.02–4.44)	1.23 ± 0.18 ^c (0.92–1.45)	1.89 ± 0.94 (0.95–3.54)	0.033
Abscess	9	2.46 ± 0.98 (1.29–3.90)	1.91 ± 1.01 (0.94–3.46)	1.44 ± 0.69 (0.84–3.05)	0.266

ARFI acoustic radiation force impulse, SWV shear wave velocity, HCC hepatocellular carcinoma, CCC cholangiocellular carcinoma, FNH focal nodular hyperplasia

^a *t* test, comparison between SWV of lesion to SWV of surrounding liver tissue

^b ANOVA test, pairwise comparison on SWV of lesion. There are statistically significant differences between the following pairs: HCC versus hemangiomas (*p* < 0.001), HCC versus focal fatty degeneration (*p* = 0.006) and metastases vs. hemangiomas (*p* < 0.001). There are no statistically significant differences between the other pairs

^c ANOVA test, pairwise comparison on SWV of surrounding liver parenchyma. There are statistically significant differences between the following pairs: surrounding liver tissue in HCC versus surrounding liver tissue in metastasis (*p* = 0.036), surrounding liver tissue in HCC versus surrounding live tissue in hemangioma (*p* < 0.001), surrounding liver tissue in HCC versus surrounding liver tissue in focal fatty degeneration (*p* < 0.001), surrounding liver tissue in HCC versus surrounding liver tissue in focal fatty sparing (*p* < 0.001) and surrounding liver tissue in HCC versus surrounding liver tissue in FNH (*p* < 0.001). There are no statistically significant differences between the other pairs

disease, and diverse degrees of background liver fibrosis, the comparative results between SWVs of HCCs and those of surrounding liver differed among studies were caused by the characteristics of each study [32, 33, 39, 40]. We found that there was statistically significant difference between the SWV value of the surrounding liver of HCC and the surrounding liver of other lesions, except the surrounding liver of CCC and abscess. The reason is that CCC, like HCC, usually combines with varying degrees of liver fibrosis as a type of primary liver cancer. There were three patients of abscess with relatively high mean SWV values (2.76, 3.44 and 3.45 m/s) of the surrounding liver tissues of lesions, which were caused by perilesional hyperemia or inflammation. These high mean SWV values affected on the statistic result. This indicates that simultaneously

measuring SWVs of FLLs and the surrounding liver should focus on evaluating the individual characteristics of the hepatic lesion and background fibrosis to prevent a misdiagnosis of the FLL using the correlation of SWVs between the hepatic lesion and surrounding liver parenchyma. Additionally, the SWVs for CCCs appeared higher than those of their surrounding liver parenchyma, but there was no significant difference between them. The reason might be the limited samples of CCCs. In this regard, a larger amount of cases would be needed in further study to prevent potential bias. The similar situation also happened in focal fatty degeneration, focal fatty sparing and liver abscess. Thus, we need to make comprehensive diagnosis by considering conventional US characteristics and clinical features as well.

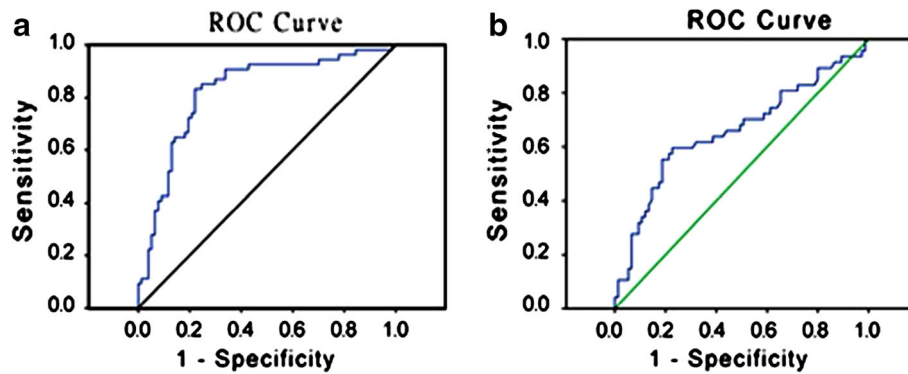
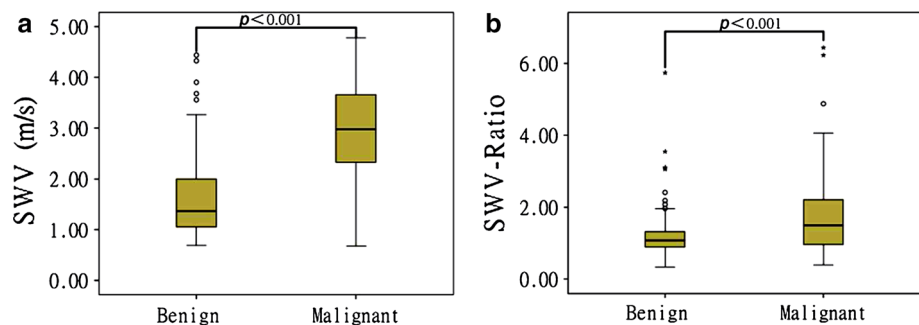


Fig. 5 ROC curve of SWVs in distinguishing malignant from benign FLLs **(a)** ROC curve of SWVs, AUROC = 0.824(95 % CI 0.748–0.899); cutoff value = 2.13 m/s; the sensitivity, specificity, PPV and NPV are 83.3, 77.9, 72.6 and 87.0 %, respectively. **(b)** ROC curve of SWV ratios, AUROC = 0.660(95 % CI 0.555–0.765); cutoff

value = 1.37; the sensitivity, specificity, PPV and NPV are 59.6, 77.3, 63.8 and 77.3 %, respectively. *ROC* receiver operating characteristics, *AUROC* area under the ROC curve, *PPV* positive predictive value, *NPV* negative predictive value

Fig. 6 SWVs of malignant masses and benign lesions. **(a)** SWV of FLL ($p < 0.001$). **(b)** SWV ratio of FLL and the surrounding liver parenchyma ($p < 0.001$). *Boxplots* with medians and quartiles (*hollow dots*) are depicted



We obtained the best cutoff value of 2.13 m/s for SWV and 1.37 for SWV ratio in diagnosing malignant liver lesions. The cutoff value for SWV was similar to most of previous reports (2.0–2.73 m/s) [27–29, 33]. However, Park et al. [32] reported the value as 1.82 m/s, which was much lower than ours and other studies. Although the cutoff value for SWV may be useful to our routine US evaluation, it should be applied cautiously in clinical practice. Our cutoff value would have a higher accuracy in identifying HCC, CCC, hemangioma, focal fatty degeneration and focal fatty sparing. However, it would mischaracterize metastasis with a relatively low SWV, or FNH and abscess with a relatively high SWV. Thus, we need to make comprehensive judgment by considering conventional US characteristics and clinical features as well. The SWV ratio of FLL to surrounding liver tissue was firstly introduced in the present study, which took into account the influence of the background liver parenchyma. However, after adding the SWV ratio for analysis, the sensitivity and specificity, respectively, decreased from 83.3 to 59.6 % and from 77.9 to 77.3 %, as compared with SWV. The findings indicate that the SWV ratio seemed to be useless in differentiating FLLs and the absolute value of SWV is more useful.

This study has several limitations. First, most patients in this study were confirmed by clinical and relevant imaging data, and only a minority of patients were definitely diagnosed by pathology. Second, the grade of hepatic parenchymal cirrhosis was not taken into consideration in the study. In addition, morphological characteristics of FLLs including size, position, boundary, shape, echogenicity and color Doppler flow image pattern were not considered in our study. Further investigation of how to evaluate morphologically varying liver lesions and their influences on SWVs should be carried out.

This study demonstrated the potential usefulness of ARFI elastography for characterization of focal liver masses. In conclusion, VTQ is a convenient and comfortable method without additional cost and is particularly suitable for the patients who are not candidates for contrast-enhanced imaging. Further studies with larger sample size would be taken to assess the usefulness of ARFI elastography in clinical practice.

Acknowledgments This work was supported in part by Grant 81371570 from National Natural Scientific Foundation of China, Grant 20114003 of Key Project from Shanghai Health Bureau and Grant 2012045 of Shanghai Talent Development Project from Shanghai Human Resource and Social Security Bureau.

Conflict of interest None.

References

- Trillaud H, Bruel JM, Valette PJ, Vilgrain V, Schmutz G, Oyen R, Jakubowski W, Danes J, Valek V, Greis C. Characterization of focal liver lesions with SonoVue to enhanced sonography: international multicenter to study in comparison to CT and MRI. *World J Gastroenterol.* 2009;15:3748–56.
- Semelka RC, Martin DR, Balci C, Lance T. Focal liver lesions: comparison of dual-phase CT and multisequence multiplanar MR imaging including dynamic gadolinium enhancement. *J Magn Reson Imaging.* 2001;13:397–401.
- Hohmann J, Albrecht T, Hoffmann CW, Wolf KJ. Ultrasonographic detection of focal liver lesions: increased sensitivity and specificity with microbubble contrast agents. *Eur J Radiol.* 2003;46:147–59.
- Xu HX, Lu MD, Liu LN, Zhang YF, Guo LH, Xu JM, Liu C. Discrimination between neoplastic and nonneoplastic lesions in cirrhotic liver using contrast-enhanced ultrasound. *Br J Radiol.* 2012;85:1376–84.
- Hargreaves BA, Worters PW, Pauly KB, Pauly JM, Koch KM, Gold GE. Metal-induced artifacts in MRI. *AJR Am J Roentgenol.* 2011;197:547–55.
- Brenner DJ, Hall EJ. Computed tomography—an increasing source of radiation exposure. *N Engl J Med.* 2007;357:2277–84.
- Wilson SR, Greenbaum LD, Goldberg BB. Contrast-enhanced ultrasound: What is the evidence and what are the obstacles? *AJR Am J Roentgenol.* 2009;193:55–60.
- Urban MW, Nenadic IZ, Chen S, Greenleaf JF. Discrepancies in reporting tissue material properties. *J Ultrasound Med.* 2013;32:886–8.
- Sarvazyan AP, Rudenko OV, Swanson SD, Fowlkes JB, Emelianov SY. Shear wave elasticity imaging: a new ultrasonic technology of medical diagnostics. *Ultrasound Med Biol.* 1998;24:1419–35.
- Zhai L, Palmeri ML, Bouchard RR, Nightingale RW, Nightingale KR. An integrated indenter-ARFI imaging system for tissue stiffness quantification. *Ultrasound Imaging.* 2008;30:95–111.
- Gallotti A, D'Onofrio M, Pozzi Mucelli R. Acoustic radiation force impulse (ARFI) technique in ultrasound with virtual touch tissue quantification of the upper abdomen. *Radiol Med.* 2010;115:889–97.
- Yu H, Wilson SR. Differentiation of benign from malignant liver masses with acoustic radiation force impulse technique. *Ultrasound Q.* 2011;27:217–23.
- Nightingale K, Soo MS, Nightingale R, Trahey G. Acoustic radiation force impulse imaging: in vivo demonstration of clinical feasibility. *Ultrasound Med Biol.* 2001;28:227–35.
- Palmeri ML, Wang MH, Dahl JJ, Frinkley KD, Nightingale KR. Quantifying hepatic shear modulus in vivo using acoustic radiation force. *Ultrasound Med Biol.* 2008;34:546–58.
- Yoon KT, Lim SM, Park JY, Kim do Y, Ahn SH, Han KH, Chon CY, Cho M, Lee JW, Kim SU. Liver stiffness measurement using acoustic radiation force impulse (ARFI) elastography and effect of necroinflammation. *Dig Dis Sci.* 2012;57:1682–91.
- D'Onofrio M, Gallotti A, Mucelli RP. Tissue quantification with acoustic radiation force impulse imaging: measurement repeatability and normal values in the healthy liver. *AJR Am J Roentgenol.* 2010;195:132–6.
- Meng W, Zhang G, Wu C, Wu G, Song Y, Lu Z. Preliminary results of acoustic radiation force impulse (ARFI) ultrasound imaging of breast lesions. *Ultrasound Med Biol.* 2011;37:1436–43.
- Zhang YF, Xu HX, He Y, Liu C, Guo LH, Liu LN, Xu JM. Virtual touch tissue quantification of acoustic radiation force impulse: a new ultrasound elastic imaging in the diagnosis of thyroid nodules. *PLoS One.* 2012;7:e49094.
- Zhang YF, He Y, Xu HX, Xu XH, Liu C, Guo LH, Liu LN, Xu JM. Virtual touch tissue imaging of acoustic radiation force impulse: a new technique in the differential diagnosis between benign and malignant thyroid nodules. *J Ultrasound Med.* 2014;33:585–95.
- Guo LH, Xu HX, Fu HJ, Peng A, Zhang YF, Liu LN. Acoustic radiation force impulse imaging for noninvasive evaluation of renal parenchyma elasticity: preliminary findings. *PLoS One.* 2013;8:e68925.
- Yashima Y, Sasahira N, Isayama H, Kogure H, Ikeda H, Hirano K, Mizuno S, Yagioka H, Kawakubo K, Sasaki T, Nakai Y, Tada M, Yoshida H, Omata M, Koike K. Acoustic radiation force impulse elastography for noninvasive assessment of chronic pancreatitis. *J Gastroenterol.* 2012;47:427–32.
- Piscaglia F, Salvatore V, Di Donato R, D'Onofrio M, Gualandi S, Gallotti A, Peri E, Borghi A, Conti F, Fattovich G, Sagrini E, Cucchetti A, Andreone P, Bolondi L. Accuracy of virtual touch acoustic radiation force impulse (ARFI) imaging for the diagnosis of cirrhosis during liver ultrasonography. *Ultraschall Med.* 2011;32:167–75.
- Palmeri ML, Wang MH, Rouze NC, Abdelmalek MF, Guy CD, Moser B, Diehl AM, Nightingale KR. Noninvasive evaluation of hepatic fibrosis using acoustic radiation force based shear stiffness in patients with nonalcoholic fatty liver disease. *J Hepatol.* 2011;55:666–72.
- Sporea I, Sirlu R, Popescu A, Danilă M. Acoustic radiation force impulse (ARFI)—a new modality for the evaluation of liver fibrosis. *Med Ultrason.* 2010;12:26–31.
- Lupsor M, Badea R, Stefanescu H, Sparchez Z, Branda H, Serban A, Maniu A. Performance of a new elastographic method (ARFI technology) compared to unidimensional transient elastography in the noninvasive assessment of chronic hepatitis C. *Preliminary results. J Gastrointest Liver Dis.* 2009;18:303–10.
- Friedrich-Rust M, Wunder K, Kriener S, Sotoudeh F, Richter S, Bojunga J, Herrmann E, Poyndar T, Dietrich CF, Vermehren J, Zeuzem S, Sarrazin C. Liver fibrosis in viral hepatitis: noninvasive assessment with acoustic radiation force impulse imaging versus transient elastography. *Radiology.* 2009;252:595–604.
- Cho SH, Lee JY, Han JK, Choi BI. Acoustic radiation force impulse elastography for the evaluation of focal solid hepatic lesions: preliminary findings. *Ultrasound Med Biol.* 2010;36:202–8.
- Davies G, Koenen M. Acoustic radiation force impulse elastography in distinguishing hepatic haemangiomas from metastases: preliminary observations. *Br J Radiol.* 2011;84:939–43.
- Shuang-Ming T, Ping Z, Ying Q, Li-Rong C, Ping Z, Rui-Zhen L. Usefulness of acoustic radiation force impulse imaging in the differential diagnosis of benign and malignant liver lesions. *Acad Radiol.* 2011;18:810–5.
- Zhang P, Zhou P, Tian SM, Qian Y, Deng J, Zhang L. Application of acoustic radiation force impulse imaging for the evaluation of focal liver lesion elasticity. *Hepatobiliary Pancreat Dis Int.* 2013;12:165–70.
- Heide R, Strobel D, Bernatik T, Goertz RS. Characterization of focal liver lesions (FLL) with acoustic radiation force impulse (ARFI) elastometry. *Ultraschall Med.* 2010;31:405–9.
- Park H, Park JY, Kim do Y, Ahn SH, Chon CY, Han KH, Kim SU. Characterization of focal liver masses using acoustic radiation force impulse elastography. *World J Gastroenterol.* 2013;19:219–26.
- Kim JE, Lee JY, Bae KS, Han JK, Choi BI. Acoustic radiation force impulse elastography for focal hepatic tumors: usefulness

- for differentiating hemangiomas from malignant tumors. *Korean J Radiol.* 2013;14:743–53.
34. Bruix J, Sherman M. Management of hepatocellular carcinoma. *Hepatology.* 2005;42:1208–36.
 35. Bruix J, Sherman M. Management of hepatocellular carcinoma: an update. *Hepatology.* 2011;53:1020–2.
 36. Hanafusa K, Ohashi I, Himeno Y, Suzuki S, Shibuya H. Hepatic hemangioma: findings with two-phase CT. *Radiology.* 1995;196:465–9.
 37. Burns PN, Wilson SR. Focal liver masses: enhancement patterns on contrast-enhanced images-concordance of US scans with CT scans and MR images. *Radiology.* 2007;242:162–74.
 38. Mattison GR, Glazer GM, Quint LE, Francis IR, Bree RL, Ensminger WD. MR imaging of hepatic focal nodular hyperplasia: characterization and distinction from primary malignant hepatic tumors. *AJR Am J Roentgenol.* 1987;148:711–5.
 39. Fahey BJ, Nelson RC, Bradway DP, Hsu SJ, Dumont DM, Trahey GE. In vivo visualization of abdominal malignancies with acoustic radiation force elastography. *Phys Med Biol.* 2008;53:279–93.
 40. DeWall RJ, Bharat S, Varghese T, Hanson ME, Agni RM, Kliever MA. Characterizing the compression-dependent viscoelastic properties of human hepatic pathologies using dynamic compression testing. *Phys Med Biol.* 2012;57:2273–86.